Acta Cryst E CRYSTALLOGRAPHIC COMMUNICATIONS

ISSN 2056-9890

Synthesis and crystal structure of γ-SrNCN at 38 GPa

Lukas Brüning,[a] Georg Krach,[b] Pascal Lennert Jurzick,[a] Wolfgang Schnick[b] and Maxim Bykov[a]*

[a]Institute for Inorganic and Analytical Chemistry, Goethe University Frankfurt, Max-von-Laue-Strasse 7, 60438 Frankfurt am Main, Germany, and [b]Department of Chemistry, University of Munich (LMU), Butenandtstrasse 5-13 (D), 81377 Munich, Germany. *Correspondence e-mail: maxim.bykov@chemie.uni-frankfurt.de

Received 1 May 2026
Accepted 9 June 2026

This article is part of the collection Early Career Scientists in Structural Science.

Keywords: crystal structure; high-pressure high-temperature synthesis; nitrides; polymorphism; carbodiimide.

CCDC reference: 2560951

Supporting information: this article has supporting information at journals.iucr.org/e

γ-Strontium carbodiimide, γ-SrNCN, was synthesized from a mixture of strontium subnitride (Sr_2N) and tetracyanoethylene (C_6N_4) at 38 (3) GPa in a laser-heated diamond anvil cell. Its crystal structure was solved and refined using synchrotron single-crystal X-ray diffraction. The new polymorph crystallizes in space group *I*4/*mcm* (No. 140), where the Sr^{2+} and NCN^{2-} packing can be derived from the CsCl (B2) structure type. γ-SrNCN (*tI*16-SrNCN) is isostructural to *tI*16-BaNCN and represents the first high-pressure polymorph of SrNCN.

1. Chemical context

Inorganic carbodiimide salts are an interesting and well-established class of materials that can exhibit exciting optical, magnetic, and catalytic properties (Corkett *et al.*, 2024). Two polymorphs of SrNCN have been reported thus far. The first characterized polymorph of strontium carbodiimide, α-SrNCN (*oP*16-SrNCN, NaSCN structure type), was synthesized through a reaction of melamine ($C_3N_6H_6$) with strontium subnitride (Sr_2N) at 1123 K (Berger & Schnick, 1994). Polycrystalline β-SrNCN (*hR*12-SrNCN, β-NaN_3 structure type) was synthesized from $SrCO_3$ in liquid NH_3 (Wissmann, 2001), while crystals suitable for single-crystal X-ray diffraction were obtained by heating reactive fluxes of SrI_2, NaCN and NaN_3 (2:1:1) at 1073 K, followed by slow cooling (Liao & Dronskowski, 2004). Krings *et al.* (2010) further expanded the range of synthetic routes to both α- and β-SrNCN and showed that β-SrNCN is the ground-state polymorph. α-SrNCN is used as a host lattice for Eu^{2+} doping, yielding an efficient orange-emitting phosphor (Krings *et al.*, 2011). Here, we report the synthesis of a high-pressure polymorph, γ-SrNCN (*tI*16-SrNCN), from a mixture of strontium subnitride (Sr_2N) and tetracyanoethylene (C_6N_4) at 38 (3) GPa. γ-SrNCN is isostructural to *tI*16-BaNCN, which is produced in a reaction of $BaCO_3$ in liquid NH_3 at ambient pressure and an elevated temperature of 1173 K (Masubuchi *et al.*, 2018). *tI*16-BaNCN remains stable upon compression up to 23 GPa. At higher pressures, it undergoes a symmetry-lowering phase transition to *mC*16-BaNCN, driven predominantly by tilting of the NCN^{2-} anions (Masubuchi *et al.*, 2022; Yamamoto *et al.*, 2026). There are a few other examples of high-pressure studies of carbodiimides (Solozhenko *et al.*, 2004; Glaser *et al.*, 2008; Möller *et al.*, 2018; Meinerzhagen *et al.*, 2024; Yang *et al.*, 2024). Furthermore, high-pressure and high-temperature conditions have proven the feasibility of synthesizing ternary nitridocarbonates with increased coordi-

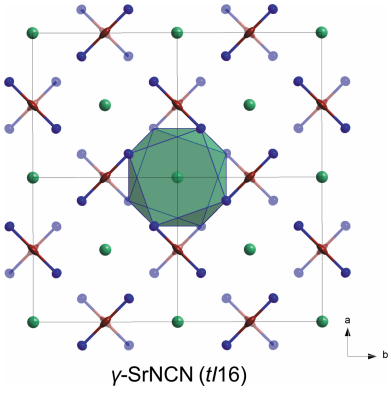

γ-SrNCN (*tI*16)

nation numbers of three and four for carbon (Brüning *et al.*, 2023; Aslandukov *et al.*, 2024).

2. Structural commentary

γ-SrNCN crystallizes in the space group *I*4/*mcm* (No. 140, KN_3 structure type), where Sr, C, and N occupy the Wyckoff positions 4*a* (site symmetry 422), 4*d* (site symmetry *m.mm*) and 8*h* (site symmetry *m*.2*m*), respectively. The bond lengths and geometry of the NCN^{2-} anion are only weakly affected by pressure, with *d*(C—N) = 1.222 (13) Å in the reported structure compared to *d*(C—N) = 1.232 (5) Å in β-SrNCN at ambient pressure. In contrast to α-SrNCN and β-SrNCN, where Sr is sixfold coordinated in an octahedral environment with *d*(Sr—N) = 2.600 (8) – 2.657 (8) Å, γ-SrNCN features Sr in an eightfold tetragonal antiprismatic coordination with *d*(Sr—N) = 2.460 (4) Å. Similar to β-SrNCN, γ-SrNCN is built from stacked layers of Sr^{2+} cations and linear NCN^{2-} anions (Fig. 1). The main difference between the polymorphs arises from the rearrangement of NCN^{2-} units: in γ-SrNCN, they are oriented parallel to the Sr^{2+} layers rather than perpendicular to them like in β-SrNCN.

Within the NCN^{2-} layers, each linear unit is rotated by 90° in the *ab* plane with respect to the corresponding unit within the adjacent layer. Treating the NCN^{2-} unit as a single pseudo-atom would result in an octahedral coordination for both Sr and NCN^{2-} in β-SrNCN, while the coordination would be cubic for γ-SrNCN. Therefore, β-SrNCN can be derived from the NaCl (B1) structure type and γ-SrNCN packing follows the CsCl (B2) structure type, consistent with the pressure-coordination rule. A parallel can be drawn to the B1 to B2 phase transition in NaCl at 30 GPa (Bassett *et al.*, 1968)

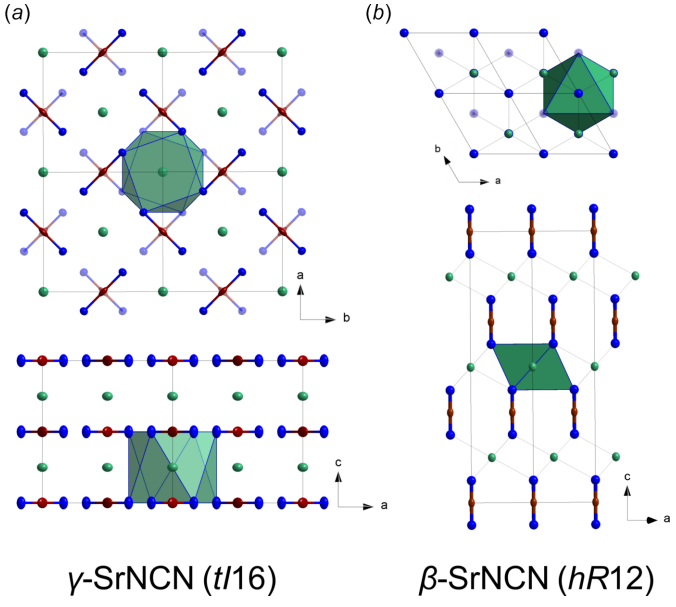

Figure 1
Crystal structure representations of (*a*) γ-SrNCN and (*b*) β-SrNCN along different crystallographic axes. Displacement ellipsoids are drawn at the 70% probability level. Sr, C and N atoms are colored green, brown and blue, respectively. Semitransparent atoms imply the next layer.

Table 1
Experimental details.

Crystal data	
Chemical formula	SrNCN
M_r	127.65
Crystal system, space group	Tetragonal, *I*4/*mcm*
Temperature (K)	293
a, *c* (Å)	5.311 (2), 5.790 (6)
V (Å^3)	163.3 (2)
Z	4
Radiation type	Synchrotron, λ = 0.2908 Å
μ (mm^{-1})	3.01
Crystal size (mm)	0.001 × 0.001 × 0.001
Data collection	
Diffractometer	Customized ω-circle diffractometer
Absorption correction	Multi-scan (*CrysAlis PRO*; Rigaku OD, 2025)
T_{min}, T_{max}	0.150, 1.000
No. of measured, independent and observed [$I > 2\sigma(I)$] reflections	366, 109, 70
R_{int}	0.072
(sin $\theta/\lambda)_{max}$ (Å^{-1})	1.006
Refinement	
$R[F^2 > 2\sigma(F^2)]$, $wR(F^2)$, *S*	0.060, 0.156, 1.15
No. of reflections	109
No. of parameters	10
$\Delta\rho_{max}$, $\Delta\rho_{min}$ (e Å^{-3})	1.97, −1.69

Computer programs: *CrysAlis PRO* (Rigaku OD, 2025), *SHELXT2014/5* (Sheldrick, 2015*a*), *SHELXL2014/7* (Sheldrick, 2015*b*) and *OLEX2* (Dolomanov *et al.*, 2009).

and to the polymorphism of NaN_3, for which the isostructural high-pressure polymorph *tI*16-NaN_3 was described (Pulham *et al.*, 2014). The results also align well with the pressure homologue rule, since CsCl (B2) packing can be achieved in *tI*16-BaNCN at ambient pressure (Masubuchi *et al.*, 2018).

3. Synthesis and crystallization

Strontium subnitride (Sr_2N) was synthesized via direct reaction of strontium metal with N_2 gas at 1273 K, as described in the literature (Reckeweg & DiSalvo, 2002). A 20 µm piece of Sr_2N was embedded in tetracyanoethylene (C_6N_4, Thermo Fischer, purity > 98%), compressed to 38 (3) GPa and laser-heated in a diamond anvil cell (BX90 body design; Boehler–Almax type diamonds with a conical aperture of 70° and 200 µm culet size) with a Nd:YAG laser (λ = 1064 nm, T > 1500 K, 4 s heating time). The same synthesis approach and detailed description of data evaluation can be found in previous works on ternary nitridocarbonates (Brüning *et al.*, 2023, 2025; Ranieri *et al.*, 2025; Jurzick *et al.*, 2026). Pressure was determined using the pressure–frequency relationship of the stressed diamond Raman band (Akahama & Kawamura, 2006). The reaction product, γ-SrNCN, was polycrystalline with submicron grain sizes, as indicated by XRD mapping of the sample chamber.

4. Refinement

Crystal data, data collection and structure refinement details are summarized in Table 1. The reaction product was studied by means of synchrotron single-crystal X-ray diffraction at the

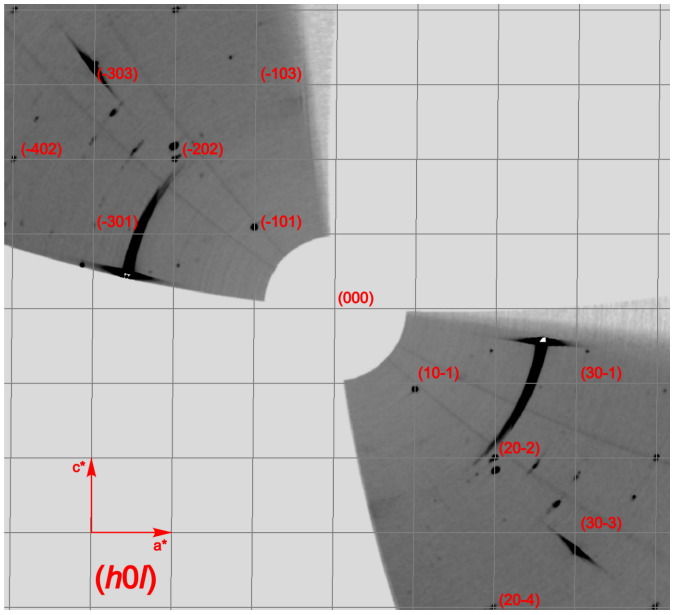

Figure 2
(*h*0*l*)-reciprocal lattice plane of γ-SrNCN (No. 140 *I*4/*mcm*) at 38 (3) GPa with indexed reflections fulfilling (*hkl*): $h + k + l = 2n$ for *I*-centering and (0*kl*): $k,l = 2n$ [$\equiv$ (*h*0*l*): $h,l = 2n$] for a *c*-glide plane perpendicular to [100] ($\equiv$ [010]).

extreme conditions beamline P02.2 at Deutsches Elektronen Synchrotron (PetraIII, DESY). The X-ray beam had a full width at half maximum of ∼2 µm and a wavelength of 0.2908 Å, and the X-ray diffraction data were measured using a PerkinElmer XRD1621 2D flat panel detector. To obtain single-crystal datasets, the diamond anvil cell was rotated around the vertical ω axis within a range of ±32°. Diffraction data were acquired in 0.5° ω steps with an exposure time of 4s per °. Data reduction was performed using *CrysAlis*^{PRO} software package. Since the dataset contains diffraction data from multiple crystallites with different orientations, the algorithm DaFi (Aslandukov *et al.*, 2022) was used to group and extract the orientation matrices from individual crystalline domains. The most prominent domain was used for integration and the resulting *hkl* file was then used for structure solution with *SHELXT* (Sheldrick 2015*a*) and refinement with *SHELXL* (Sheldrick 2015*b*) within the *OLEX2-1.5* interface (Dolomanov *et al.*, 2009). The limited opening of the diamond anvil cell results in reduced completeness of the datasets. As a standard procedure, we carefully examine reconstructed precession images of each dataset to check for missing superlattice reflections and to cross-check the choice of the space-group symmetry. In the case of γ-SrNCN, the systematic absences are consistent with the *I*4/*mcm* space group. It can be shown that (0*kl*): $k,l = 2n$ [$\equiv$(*h*0*l*): $h,l = 2n$] for a *c*-glide plane perpendicular to [100] ($\equiv$[010]) in a tetragonal body-centered Bravais lattice holds (Fig. 2).

Acknowledgements

We acknowledge the Deutsches Elektronen Synchrotron (DESY) for provision of synchrotron radiation facilities and we would like to thank Dr Nico Giordano for assistance and support in using beamline P02.2.

Funding information

Funding for this research was provided by: Deutsche Forschungsgemeinschaft (grant No. BY112/2-1 to Maxim Bykov).

References

Akahama, Y. & Kawamura, H. (2006). *J. Appl. Phys.* **100**, 043516.
Aslandukov, A., Aslandukov, M., Dubrovinskaia, N. & Dubrovinsky, L. (2022). *J. Appl. Cryst.* **55**, 1383–1391.
Aslandukov, A., Liang, A., Ehn, A., Trybel, F., Yin, Y., Aslandukova, A., Akbar, F. I., Ranieri, U., Spender, J., Howie, R. T., Bright, E. L., Wright, J., Hanfland, M., Garbarino, G., Mezouar, M., Fedotenko, T., Abrikosov, I. A., Dubrovinskaia, N., Dubrovinsky, L. & Laniel, D. (2024). *J. Am. Chem. Soc.* **146**, 18161–18171.
Bassett, W. A., Takahashi, T., Mao, H.-K. & Weaver, J. S. (1968). *J. Appl. Phys.* **39**, 319–325.
Berger, U. & Schnick, W. (1994). *J. Alloys Compd.* **206**, 179–184.
Brüning, L., Jena, N., Bykova, E., Jurzick, P. L., Flosbach, N. T., Mezouar, M., Hanfland, M., Giordano, N., Fedotenko, T., Winkler, B., Abrikosov, I. A. & Bykov, M. (2023). *Angew. Chem. Int. Ed.* **62**, e202311519.
Brüning, L., Jena, N., Jurzick, P. L., Bykova, E., Giordano, N., Mezouar, M., Abrikosov, I. A. & Bykov, M. (2025). *Angew. Chem. Int. Ed.* **64**, e202506406.
Corkett, A. J., Reckeweg, O., Pöttgen, R. & Dronskowski, R. (2024). *Chem. Mater.* **36**, 9107–9125.
Dolomanov, O. V., Bourhis, L. J., Gildea, R. J., Howard, J. A. K. & Puschmann, H. (2009). *J. Appl. Cryst.* **42**, 339–341.
Glaser, J., Unverfehrt, L., Bettentrup, H., Heymann, G., Huppertz, H., Jüstel, T. & Meyer, H.-J. (2008). *Inorg. Chem.* **47**, 10455–10460.
Jurzick, P. L., Brüning, L., Winkler, B., Wang, Y., Dronskowski, R., Bykova, E., Spahr, D., Hanfland, M., Wehinger, B., Giordano, N. & Bykov, M. (2026). *J. Am. Chem. Soc.* **148**, 2843–2850.
Krings, M., Montana, G., Dronskowski, R. & Wickleder, C. (2011). *Chem. Mater.* **23**, 1694–1699.
Krings, M., Wessel, M., Wilsmann, W., Müller, P. & Dronskowski, R. (2010). *Inorg. Chem.* **49**, 2267–2272.
Liao, W. & Dronskowski, R. (2004). *Acta Cryst.* E**60**, i124–i126.
Masubuchi, Y., Miyazaki, S., Song, P., Yamamoto, T., Nakano, K., Hongo, K. & Maezono, R. (2022). *J. Alloys Compd.* **918**, 165632.
Masubuchi, Y., Nishitani, S., Hosono, A., Kitagawa, Y., Ueda, J., Tanabe, S., Yamane, H., Higuchi, M. & Kikkawa, S. (2018). *J. Mater. Chem. C.* **6**, 6370–6377.
Meinerzhagen, Y., Eickmeier, K., Müller, P. C., Hempelmann, J., Houben, A. & Dronskowski, R. (2024). *J. Appl. Cryst.* **57**, 1436–1445.
Möller, A., Konze, P. M. & Dronskowski, R. (2018). *Z. Anorg. Allg. Chem.* **644**, 1881–1885.
Pulham, Millar, Barry, & Marshall (2014). *Z. Krist. Cryst. Mater.* **229**, 259–275.
Ranieri, U., Liang, A., Lamb, C., Spender, J., Bolton, S., Aslandukov, A., Massani, B., Tasnádi, F., Autran, P.-O., Ball, J. A. D., Rosa, A. D., Wang, B., Trybel, F. & Laniel, D. (2025). *J. Am. Chem. Soc.* **147**, 35431–35437.
Reckeweg, O. & DiSalvo, F. J. (2002). *Solid State Sci.* **4**, 575–584.
Rigaku OD (2025). *CrysAlis*^{PRO}. Rigaku Oxford Diffraction, Yarnton, England.
Sheldrick, G. M. (2015*a*). *Acta Cryst.* A**71**, 3–8.

Sheldrick, G. M. (2015*b*). *Acta Cryst.* C**71**, 3–8.
Solozhenko, V. L., Schwarz, M. & Riedel, R. (2004). *Solid State Commun.* **132**, 573–576.
Wissmann, B. (2001). Dissertation, Universität Tübingen, Germany.
Yamamoto, Y., Kume, K., Shinozaki, A., Ichibha, T., Hongo, K., Miura, A. & Masubuchi, Y. (2026). *Solid State Sci.* **173**, 108188.
Yang, Z., Wu, B., Niu, S., Zhai, C., Xu, T., Dang, L., Qi, X., Liu, X., Shi, R., Ma, S. & Yao, M. (2024). *Chem. Phys. Lett.* **840**, 141142.

supporting information

Acta Cryst. (2026). E**82**, 764-767 [https://doi.org/10.1107/S2056989026006080]

Synthesis and crystal structure of γ-SrNCN at 38 GPa

Lukas Brüning, Georg Krach, Pascal Lennert Jurzick, Wolfgang Schnick and Maxim Bykov

Computing details

γ-Strontium carbodiimide

Crystal data

SrNCN
M_r = 127.65
Tetragonal, *I*4/*mcm*
a = 5.311 (2) Å
c = 5.790 (6) Å
V = 163.3 (2) Å^3
Z = 4
F(000) = 232
D_x = 5.191 Mg m^{-3}
Synchrotron radiation, λ = 0.2908 Å
Cell parameters from 94 reflections
θ = 2.2–14.7°
μ = 3.01 mm^{-1}
T = 293 K
Irregular, dull dark gray
0.001 × 0.001 × 0.001 mm

Data collection

Customized ω-circle diffractometer
Radiation source: synchrotron, PETRAIII, Beamline P02.2
Synchrotron monochromator
Detector resolution: 5.0 pixels mm^{-1}
ω scans
Absorption correction: multi-scan (CrysAlisPro; Rigaku OD, 2025)
T_{min} = 0.150, T_{max} = 1.000
366 measured reflections
109 independent reflections
70 reflections with $I > 2\sigma(I)$
R_{int} = 0.072
θ_{max} = 17.0°, θ_{min} = 3.6°
h = −7→7
k = −8→7
l = −7→8

Refinement

Refinement on F^2
Least-squares matrix: full
$R[F^2 > 2\sigma(F^2)]$ = 0.060
$wR(F^2)$ = 0.156
S = 1.15
109 reflections
10 parameters
0 restraints
Primary atom site location: dual
$w = 1/[\sigma^2(F_o^2) + (0.0651P)^2]$ where $P = (F_o^2 + 2F_c^2)/3$
$(\Delta/\sigma)_{max} < 0.001$
$\Delta\rho_{max}$ = 1.97 e Å^{-3}
$\Delta\rho_{min}$ = −1.69 e Å^{-3}

Special details

Experimental. X-ray diffraction was measured at 38 (3) GPa on synthesis products, produced by laser-heating in a diamond anvil cell with an opening angle of 70°. Tetracyanoethylene was used as the pressure-transmitting medium. Pressure was determined using the pressure-frequency relationship of the stressed diamond Raman band.

Geometry. All esds (except the esd in the dihedral angle between two l.s. planes) are estimated using the full covariance matrix. The cell esds are taken into account individually in the estimation of esds in distances, angles and torsion angles; correlations between esds in cell parameters are only used when they are defined by crystal symmetry. An approximate (isotropic) treatment of cell esds is used for estimating esds involving l.s. planes.

Fractional atomic coordinates and isotropic or equivalent isotropic displacement parameters (Å²)

	x	*y*	*z*	U_{iso}*/U_{eq}
Sr01	0.5000	0.5000	0.2500	0.0118 (5)
C1	0.5000	0.0000	0.0000	0.012 (3)
N1	0.3373 (18)	0.1627 (18)	0.0000	0.013 (2)

Atomic displacement parameters (Å²)

	U^{11}	U^{22}	U^{33}	U^{12}	U^{13}	U^{23}
Sr01	0.0132 (6)	0.0132 (6)	0.0092 (11)	0.000	0.000	0.000
C1	0.012 (5)	0.012 (5)	0.013 (11)	−0.008 (6)	0.000	0.000
N1	0.009 (3)	0.009 (3)	0.019 (8)	0.001 (4)	0.000	0.000

Geometric parameters (Å, º)

Sr01—Sr01^{i}	2.895 (3)	C1—Sr01^{ix}	3.0245 (11)
Sr01—Sr01^{ii}	2.895 (3)	C1—Sr01^{x}	3.0245 (11)
Sr01—C1^{iii}	3.0245 (11)	C1—Sr01^{xi}	3.0245 (11)
Sr01—C1	3.0245 (11)	C1—Sr01^{vii}	3.0245 (11)
Sr01—N1^{iv}	2.460 (4)	C1—Sr01^{xii}	3.0245 (11)
Sr01—N1^{v}	2.460 (4)	C1—Sr01^{i}	3.0245 (11)
Sr01—N1	2.460 (4)	C1—Sr01^{xiii}	3.0245 (11)
Sr01—N1^{vi}	2.460 (4)	C1—N1	1.222 (13)
Sr01—N1^{i}	2.460 (4)	C1—N1^{xii}	1.222 (13)
Sr01—N1^{vii}	2.460 (4)	N1—Sr01^{xi}	2.460 (4)
Sr01—N1^{iii}	2.460 (4)	N1—Sr01^{vii}	2.460 (4)
Sr01—N1^{viii}	2.460 (4)	N1—Sr01^{i}	2.460 (4)
Sr01^{ii}—Sr01—Sr01^{i}	180.0	N1^{viii}—Sr01—N1^{vi}	86.5 (5)
Sr01^{ii}—Sr01—C1	118.59 (3)	N1^{iv}—Sr01—N1^{v}	149.1 (6)
Sr01^{i}—Sr01—C1^{iii}	118.59 (3)	N1^{iii}—Sr01—N1^{vii}	69.74 (7)
Sr01^{i}—Sr01—C1	61.41 (3)	N1—Sr01—N1^{vi}	69.74 (7)
Sr01^{ii}—Sr01—C1^{iii}	61.41 (3)	N1^{iv}—Sr01—N1^{iii}	80.5 (2)
C1—Sr01—C1^{iii}	180.0	Sr01—C1—Sr01^{xi}	103.24 (2)
N1^{viii}—Sr01—Sr01^{i}	126.04 (7)	Sr01^{xii}—C1—Sr01^{vii}	103.24 (2)
N1^{iv}—Sr01—Sr01^{ii}	126.04 (7)	Sr01^{vii}—C1—Sr01^{x}	180.0
N1^{iii}—Sr01—Sr01^{ii}	53.96 (7)	Sr01^{xi}—C1—Sr01^{vii}	57.19 (5)
N1—Sr01—Sr01^{i}	53.96 (7)	Sr01^{ix}—C1—Sr01^{x}	57.19 (5)
N1—Sr01—Sr01^{ii}	126.04 (7)	Sr01^{xiii}—C1—Sr01^{x}	103.24 (2)
N1^{iv}—Sr01—Sr01^{i}	53.96 (7)	Sr01^{ix}—C1—Sr01^{vii}	122.81 (5)
N1^{vi}—Sr01—Sr01^{i}	53.96 (7)	Sr01^{ix}—C1—Sr01^{xi}	180.0
N1^{i}—Sr01—Sr01^{i}	53.96 (7)	Sr01^{i}—C1—Sr01^{vii}	103.24 (2)
N1^{viii}—Sr01—Sr01^{ii}	53.96 (7)	Sr01—C1—Sr01^{x}	103.24 (2)
N1^{i}—Sr01—Sr01^{ii}	126.04 (7)	Sr01^{xii}—C1—Sr01^{x}	76.76 (2)
N1^{vii}—Sr01—Sr01^{ii}	53.96 (7)	Sr01—C1—Sr01^{xii}	180.0
N1^{vi}—Sr01—Sr01^{ii}	126.04 (7)	Sr01—C1—Sr01^{ix}	76.76 (2)
N1^{vii}—Sr01—Sr01^{i}	126.04 (7)	Sr01—C1—Sr01^{vii}	76.76 (2)

N1^{v}—Sr01—Sr01^{i}	126.04 (7)	Sr01^{xi}—C1—Sr01^{xiii}	103.24 (2)
N1^{v}—Sr01—Sr01^{ii}	53.96 (7)	Sr01^{i}—C1—Sr01^{x}	76.76 (2)
N1^{iii}—Sr01—Sr01^{i}	126.04 (7)	Sr01^{xii}—C1—Sr01^{xiii}	57.19 (5)
N1^{i}—Sr01—C1	110.97 (18)	Sr01^{xiii}—C1—Sr01^{vii}	76.76 (2)
N1^{vii}—Sr01—C1^{iii}	91.5 (2)	Sr01—C1—Sr01^{i}	57.19 (5)
N1^{iii}—Sr01—C1	157.1 (3)	Sr01^{xi}—C1—Sr01^{xii}	76.76 (2)
N1^{iii}—Sr01—C1^{iii}	22.9 (3)	Sr01^{ix}—C1—Sr01^{i}	103.24 (2)
N1^{viii}—Sr01—C1^{iii}	53.8 (3)	Sr01^{xi}—C1—Sr01^{x}	122.81 (5)
N1^{vii}—Sr01—C1	88.5 (2)	Sr01^{xi}—C1—Sr01^{i}	76.76 (2)
N1^{i}—Sr01—C1^{iii}	69.03 (18)	Sr01—C1—Sr01^{xiii}	122.81 (5)
N1^{vi}—Sr01—C1	53.8 (3)	Sr01^{xii}—C1—Sr01^{i}	122.81 (5)
N1^{viii}—Sr01—C1	126.2 (3)	Sr01^{xiii}—C1—Sr01^{i}	180.0
N1^{vi}—Sr01—C1^{iii}	126.2 (3)	Sr01^{ix}—C1—Sr01^{xiii}	76.76 (2)
N1—Sr01—C1^{iii}	157.1 (3)	Sr01^{ix}—C1—Sr01^{xii}	103.24 (2)
N1^{v}—Sr01—C1	69.03 (18)	N1^{xii}—C1—Sr01^{vii}	128.380 (11)
N1—Sr01—C1	22.9 (3)	N1^{xii}—C1—Sr01^{i}	128.380 (11)
N1^{iv}—Sr01—C1^{iii}	88.5 (2)	N1—C1—Sr01^{xii}	128.380 (11)
N1^{iv}—Sr01—C1	91.5 (2)	N1—C1—Sr01^{x}	128.380 (11)
N1^{v}—Sr01—C1^{iii}	110.97 (18)	N1^{xii}—C1—Sr01^{ix}	51.620 (11)
N1^{viii}—Sr01—N1^{i}	80.5 (2)	N1^{xii}—C1—Sr01^{xii}	51.620 (11)
N1^{vi}—Sr01—N1^{v}	80.5 (2)	N1^{xii}—C1—Sr01	128.380 (11)
N1—Sr01—N1^{v}	86.5 (5)	N1—C1—Sr01^{vii}	51.620 (11)
N1^{i}—Sr01—N1^{v}	138.9 (5)	N1—C1—Sr01^{xiii}	128.380 (11)
N1^{viii}—Sr01—N1^{iii}	69.74 (7)	N1—C1—Sr01^{i}	51.620 (11)
N1^{viii}—Sr01—N1^{vii}	107.91 (13)	N1^{xii}—C1—Sr01^{xi}	128.380 (11)
N1^{vii}—Sr01—N1^{v}	69.74 (7)	N1—C1—Sr01^{ix}	128.380 (11)
N1—Sr01—N1^{i}	107.91 (13)	N1^{xii}—C1—Sr01^{x}	51.620 (11)
N1^{viii}—Sr01—N1^{iv}	138.9 (5)	N1—C1—Sr01	51.620 (11)
N1—Sr01—N1^{iv}	69.74 (7)	N1^{xii}—C1—Sr01^{xiii}	51.620 (11)
N1^{viii}—Sr01—N1^{v}	69.74 (7)	N1—C1—Sr01^{xi}	51.620 (11)
N1^{iv}—Sr01—N1^{i}	69.74 (7)	N1^{xii}—C1—N1	180.0 (13)
N1^{iv}—Sr01—N1^{vii}	86.5 (5)	Sr01—N1—Sr01^{i}	72.09 (13)
N1^{iii}—Sr01—N1^{v}	107.91 (13)	Sr01^{xi}—N1—Sr01	149.1 (6)
N1^{iv}—Sr01—N1^{vi}	107.91 (13)	Sr01^{xi}—N1—Sr01^{i}	99.5 (2)
N1^{iii}—Sr01—N1^{i}	86.5 (5)	Sr01^{xi}—N1—Sr01^{vii}	72.09 (13)
N1^{iii}—Sr01—N1^{vi}	149.1 (6)	Sr01—N1—Sr01^{vii}	99.5 (2)
N1^{viii}—Sr01—N1	149.1 (6)	Sr01^{vii}—N1—Sr01^{i}	149.1 (6)
N1^{vii}—Sr01—N1^{vi}	138.9 (5)	C1—N1—Sr01^{i}	105.5 (3)
N1^{vii}—Sr01—N1^{i}	149.1 (6)	C1—N1—Sr01^{xi}	105.5 (3)
N1^{i}—Sr01—N1^{vi}	69.74 (7)	C1—N1—Sr01^{vii}	105.5 (3)
N1—Sr01—N1^{iii}	138.9 (5)	C1—N1—Sr01	105.5 (3)
N1—Sr01—N1^{vii}	80.5 (2)		

Sr01—C1—N1—Sr01^{xi}	180.000 (1)	Sr01^{ix}—C1—N1—Sr01	0.000 (1)
Sr01^{xii}—C1—N1—Sr01^{vii}	75.25 (6)	Sr01^{xiii}—C1—N1—Sr01^{xi}	−75.25 (6)
Sr01^{xiii}—C1—N1—Sr01^{i}	180.0	Sr01^{xi}—C1—N1—Sr01	180.0
Sr01^{xi}—C1—N1—Sr01^{vii}	75.25 (6)	Sr01^{xiii}—C1—N1—Sr01^{vii}	0.0
Sr01—C1—N1—Sr01^{i}	75.25 (6)	Sr01^{xii}—C1—N1—Sr01	180.0

Sr01^{xii}—C1—N1—Sr01^{i}	−104.75 (6)	Sr01^{i}—C1—N1—Sr01^{xi}	104.75 (6)
Sr01^{ix}—C1—N1—Sr01^{vii}	−104.75 (6)	Sr01^{xiii}—C1—N1—Sr01	104.75 (6)
Sr01^{ix}—C1—N1—Sr01^{xi}	180.0	Sr01^{ix}—C1—N1—Sr01^{i}	75.25 (6)
Sr01^{i}—C1—N1—Sr01^{vii}	180.0	Sr01^{i}—C1—N1—Sr01	−75.25 (6)
Sr01^{x}—C1—N1—Sr01^{vii}	180.0	Sr01^{vii}—C1—N1—Sr01^{xi}	−75.25 (6)
Sr01^{xi}—C1—N1—Sr01^{i}	−104.75 (6)	Sr01^{vii}—C1—N1—Sr01	104.75 (6)
Sr01^{xii}—C1—N1—Sr01^{xi}	0.000 (1)	Sr01^{vii}—C1—N1—Sr01^{i}	180.0
Sr01^{x}—C1—N1—Sr01^{i}	0.000 (1)	Sr01^{x}—C1—N1—Sr01	−75.25 (6)
Sr01—C1—N1—Sr01^{vii}	−104.75 (6)	Sr01^{x}—C1—N1—Sr01^{xi}	104.75 (6)

Symmetry codes: (i) −*x*+1, −*y*+1, −*z*; (ii) −*x*+1, −*y*+1, −*z*+1; (iii) −*y*+1/2, *x*+1/2, *z*+1/2; (iv) *y*, −*x*+1, −*z*; (v) *y*+1/2, −*x*+1/2, −*z*+1/2; (vi) −*y*+1, *x*, *z*; (vii) −*x*+1/2, −*y*+1/2, −*z*+1/2; (viii) *x*+1/2, *y*+1/2, *z*+1/2; (ix) −*x*+3/2, −*y*+1/2, −*z*+1/2; (x) *x*+1/2, *y*−1/2, *z*−1/2; (xi) *x*−1/2, *y*−1/2, *z*−1/2; (xii) −*x*+1, −*y*, −*z*; (xiii) *x*, *y*−1, *z*.